

SAND REPORT

SAND2002-8311
Unlimited Release
Printed July 2002

Effect of Substrate Configuration on the Grain Structure and Morphology of Electrodeposited Ni for Prototyping LIGA

N. Y. C. Yang and J. J. Kelly

Prepared by
Sandia National Laboratories
Albuquerque, New Mexico 87185 and Livermore, California 94550

Sandia is a multiprogram laboratory operated by Sandia Corporation, a Lockheed Martin Company, for the United States Department of Energy under Contract DE-AC04-94AL85000.

Approved for public release; further dissemination unlimited.



Issued by Sandia National Laboratories, operated for the United States Department of Energy by Sandia Corporation.

NOTICE: This report was prepared as an account of work sponsored by an agency of the United States Government. Neither the United States Government, nor any agency thereof, nor any of their employees, nor any of their contractors, subcontractors, or their employees, make any warranty, express or implied, or assume any legal liability or responsibility for the accuracy, completeness, or usefulness of any information, apparatus, product, or process disclosed, or represent that its use would not infringe privately owned rights. Reference herein to any specific commercial product, process, or service by trade name, trademark, manufacturer, or otherwise, does not necessarily constitute or imply its endorsement, recommendation, or favoring by the United States Government, any agency thereof, or any of their contractors or subcontractors. The views and opinions expressed herein do not necessarily state or reflect those of the United States Government, any agency thereof, or any of their contractors.

Printed in the United States of America. This report has been reproduced directly from the best available copy.

Available to DOE and DOE contractors from
U.S. Department of Energy
Office of Scientific and Technical Information
P.O. Box 62
Oak Ridge, TN 37831

Telephone: (865) 576-8401
Facsimile: (865) 576-5728
E-Mail: reports@adonis.osti.gov
Online ordering: <http://www.doe.gov/bridge>

Available to the public from
U.S. Department of Commerce
National Technical Information Service
5285 Port Royal Rd
Springfield, VA 22161

Telephone: (800) 553-6847
Facsimile: (703) 605-6900
E-Mail: orders@ntis.fedworld.gov
Online order: <http://www.ntis.gov/ordering.htm>



SAND2002-8311
Unlimited Release
Printed July 2002

EFFECT OF SUBSTRATE CONFIGURATION ON THE GRAIN STRUCTURE AND MORPHOLOGY OF ELECTRODEPOSITED NI FOR PROTOTYPING LIGA

Nancy Y. C. Yang
Analytical Materials Science Department 8723

James J. Kelly
Microsystems Department 8729
Sandia National Laboratories, California

ABSTRACT

Synchrotron X-ray lithographic molding of PMMA-Ti/Cu/Ti substrates has been developed and used in the electrodeposition of Ni microparts for prototype LIGA development at SNL, CA. Alternative molding processes that minimize x-ray beam line use and reduce processing time are of interest for the rapid fabrication of large quantities of microparts. The objective of this investigation is to examine, archive, and compare the grain structure and morphology of deposits produced from four different molding technologies currently under development. We conclude that deposit microstructure and uniformity are greatly influenced by substrate material and design configuration. The findings are summarized below.

Deposit Type I [standard LIGA process] (PMMA - planar Ti/Cu/Ti substrate):

- Deposition is unidirectional toward the top surface and 100% dense. Comprised of columnar grains with the long axis parallel to the plating direction. Microstructure in general is uniform throughout deposit.

Deposit Type II (PMMA - planar steel microscreen substrate):

- Deposition is also unidirectional with some perturbation above the 100 μm holes. The Ni is generally dense and contains columnar grains. Microstructure is non-uniform. Presence of holes in the substrate produced an array of cylindrical hole-affected-zones (HAZ) that contain radially distributed columnar grains with center pinholes.

Deposit Type III (3-dimensional Ni-replication substrate):

- Deposition is multi-directional. The deposits contain columnar grain cells with different orientations depending on the wall location. Voiding may occur near the center of the feature; this is attributed to premature closure of the top mold openings when pulse-plating parameters are not optimal.

Deposit Type IV (3-D Ag fiber-filled PMMA composite substrate):

- The substrate is porous and discontinuous. Microstructure of deposit is non-uniform and unpredictable. It is greatly affected by sidewall morphology, roughness, local Ag-fiber density, and the presence of open pores. The deposits may also exhibit voiding for the same reason as deposit Type III.

It should be kept in mind that the metallurgical characteristics described above were generated from limited samples from the still-evolving processes. Nonetheless, the results should provide valuable technical insight for subsequent molding/electroplating process development and optimization in Sandia National Laboratories, California.

Acknowledgment

The authors would like to thank John Hachman for his assistance with the electroplating, Andy Gardea for the optical metallography, and Chris Adcock, Ja Lee Yio, and Jeff Chames for the electron microscopy. Linda Domeier and Alf Morales are greatly appreciated for the technical discussions and valuable comments on the manuscript. The authors would also like to thank both Jill Hruby and Craig Henderson for providing the resource and support for these projects.

This page intentionally left blank.

TABLE OF CONTENTS

	<u>Page No.</u>
I. Introduction	7
II. Experimental Procedure	8
Material	8
Sample Preparation	8
Microstructural Examination	8
III. Results and Discussion	10
Deposit Type I (PMMA Mold: Planar Ti/Cu/Ti Substrates)	10
Deposit Type II (PMMA Mold: Planar Steel Microscreen Substrate)	10
Deposit Type III (3-Dimensional Ni Replication Mold/Substrate)	12
Deposit Type IV (3-Dimensional Ag-Fiber-PMMA Mold/Substrate)	13
IV. Summary	14
V. Conclusions	15
References	16
Figures	17-35

This page intentionally left blank.

EFFECT OF SUBSTRATE CONFIGURATION ON THE GRAIN STRUCTURE AND MORPHOLOGY OF ELECTRODEPOSITED NI FOR PROTOTYPING LIGA

I. Introduction

X-ray lithography molding of PMMA-Ti/Cu/Ti substrates play a central role in the current prototype LIGA¹ development program at Sandia National Laboratories, California. The process has been developed and used for some years. Nonetheless, alternative process routes that minimize or exclude the x-ray exposure step are still of interest, particularly in cases where large quantities of inexpensive microparts are desired. These alternative molding process research efforts may lead to processes that are potentially more economical and efficient compared to conventional x-ray lithographic molding. A more general, important long-term goal of the LIGA technology development program is the fabrication of high aspect ratio, micro-sized structures that meet high material performance requirements. Any viable molding process being developed should not only be efficient and economical but capable of producing structures that possess required metallurgical characteristics. The microstructure, mechanical properties, texture, and micro hardness of the Ni electrodeposits from the PMMA-Ti/Cu/Ti substrates have been studied (Ref. 1, 2) and well characterized. The main objective of the current study is to evaluate, archive, and compare Ni electroplated from three alternative molding processes with that resulting from standard PMMA-Ti/Cu/Ti substrates. The results will bring some insight to the on-going molding/electroplating process development in Sandia National Laboratories, California.

¹ LIGA is a German acronym for lithography, electroplating, and molding.

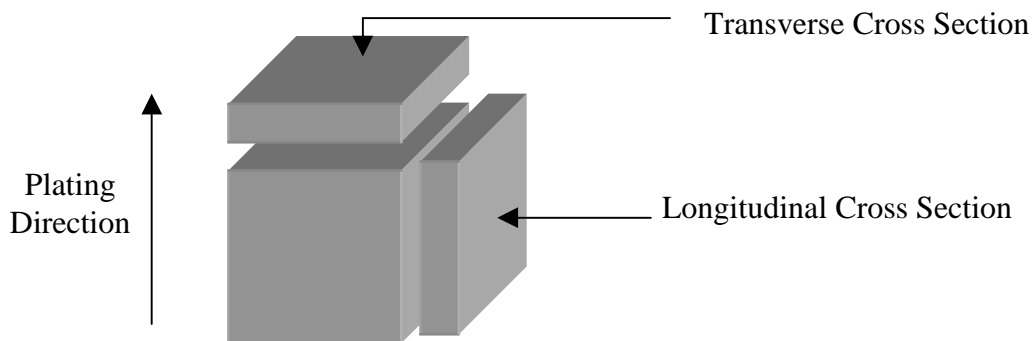
II. Experimental Procedure

Material

Materials used in the current studies are described in the following Table I.

Sample Preparation

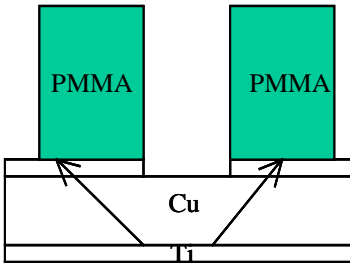
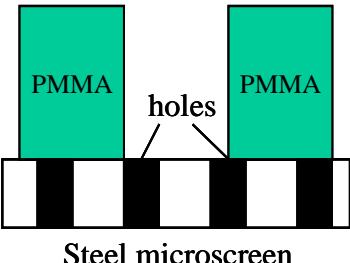
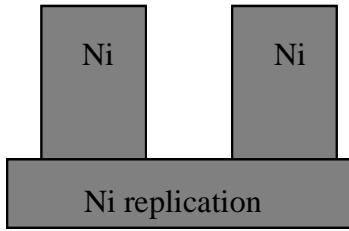
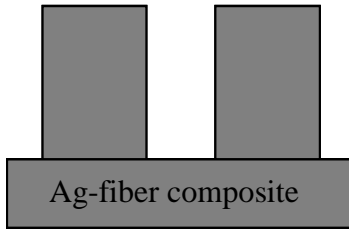
Transverse and longitudinal cross sections were sliced from the deposit with or without substrates as shown in the schematic. The cross-sectional surfaces were ground and polished using standard metallographic techniques. Samples were sequentially ground with 200, 400, 600 grit SiC papers followed by 6, 2, and 1 μm Al_2O_3 slurries. The surface at the end of the process was scratch-free and mirror finish in quality.



Microstructural Examination

Overall deposit integrity was examined using a Leitz optical microscope equipped with a digital capturing system (S-3M0) and JEOL 840 and 6400F scanning electron microscopes using secondary electron images (SEM/SEI). Film microstructure, grain size and morphology were further examined via SEM with backscattered electron images (SEM/BEI). The two SEM/BEI/SEI systems were used interchangeably.

Table I: Materials

	Deposit # I on 2-D TiCuTi	Deposit # II on 2-D Steel microscreen	Deposit # III on 3-D Ni replica	Deposit # IV on 3-D Ag fiber composite
AR-samples	under-plated ESD shuttle in the PMMA mold & released baseline Ni gear	-Unreleased electrodeposits on the steel microscreen - released and lapped gear	electrodeposits in the Ni-mold	Underplated deposits in the Ag-composite mold
Plating conditions	15mA/cm ²	15mA/cm ²	15mA/cm ²	Pulse plated
Molding & substrate material	PMMA on 0.4μm The Ti/Cu/Ti film	PMMA on steel microscreen with array 100um holes	100% dense Ni-metal	20% Vol % silver fiber-filled PMMA composite
Substrate configuration	2-D, continuous TiCuTi at the bottom	2-D, Planar, discontinuous Steel microscreen at the bottom	3-D continuous Ni metal	3-D, discontinuous & porous Ag-fiber PMMA composite
Molding technique	X-ray lithography	Injection molding	Ni replication	Mechanical drilling
Construction schematic				

III. Results and Discussion

Deposit Type I [standard LIGA process] (PMMA Mold: *Planar Ti/Cu/Ti Substrate*)

Typical electroplated, released and lapped LIGA microsystems, e.g., a gear and an environmental sensing device (ESD) shuttle, are shown in Figure 1a-b.

An underplated ESD shuttle in the PMMA and released gear were used to evaluate overall deposit integrity and microstructure, respectively. Optical images (Figure 2a-b) from a longitudinal cross section of an underplated shuttle shows that deposition is unidirectional. The deposit surface is relatively flat and uniform in thickness before reaching the top mold surface (Figure 2). This is true for both high and low aspect ratio parts. The deposit is 100% dense with no evidence of voiding.

The microstructure of a lapped/released gear was examined using SEM/BEI. A longitudinal section show that the grains are columnar ($<0.3 \mu\text{m}$ wide) with aspect ratios greater than 5. The long axis of the columnar grains is parallel to the plating direction, shown in Figure 3a-b.

The grain morphology and size are generally consistent throughout the part. In some cases, a slight increase in grain size may be seen (Figure 4).

The transverse section shows that the grains are equiaxed in the plane perpendicular to the plating direction (Figure 5a-b). The microstructure of this prototype LIGA Ni-deposit has been studied further by Yang and Kelly (Ref. 1).

Deposit Type II (PMMA Mold: *Planar Steel Microscreen Substrate*)

Typical test patterns produced from the steel microscreen substrate early in FY01 are shown in Figure 6a-b (Ref. 3). The underplated and unreleased test pattern was used in studying and evaluating the microstructure. A typical underplated and unreleased pattern is shown in Figure 6a. The steel microscreen substrate contains an array of insulating holes ($\sim 100 \mu\text{m}$ in diameter).

A longitudinal section of the underplated parts show that the deposition above the steel substrate material is unidirectional toward the mold surface and that the deposit is uniform in thickness (Figure 7a). But above the microscreen holes,

the deposit thickness is not uniform. The deposit surface is concave toward the center of the screen hole as shown in Figure 7b. The same longitudinal cross-section shows that the deposit is 100% dense throughout the part dimension. Cracks are found at several points along the deposit/substrate interface, primarily around the edge of the holes (Figure 7a-b). On the as-plated transverse surface of the same underplated part, an array of dimples was seen on the top surface above the holes (Figure 8a). The dimple array layout appears to be a direct reflection of the hole array from the substrate. On the released etched (bottom) side of the fully plated/lapped/released gear, an array of circular disks were seen with a spacing similar to that of the microscreen holes (Figure 8b). Within the disks, coarse radial features, presumably columnar grains, and a pinhole ($>10\ \mu\text{m}$) in the middle are visible (Figure 8c).

High magnification SEM-BEI images of longitudinal section show that the grains above the steel substrate are columnar with their long axis parallel to the plating direction (Figure 9a-c). This is similar to those seen on the PMMA-Ti/Cu/Ti substrate described above. The grain size increase toward the top is evident throughout the part. The grain structure above the holes is very different from that above the steel substrate. There are clearly areas above the microscreen holes where the film growth is no longer unidirectional towards the plating direction. The long axes of those grains near the holes (the hole-affected zones, or HAZ) slant gradually toward the adjacent holes to fill the gap, and the surface is concave. The depth of the depression is highly dependent on its distance from the center of the hole (Figure 9b-c). In some cases, the grains seen in the center of the HAZ appear to be equiaxed in the longitudinal section. This is an orientation artifact due to cross section of columnar grains facing towards the front. The HAZ grain structure appears to extend throughout the entire thickness.

SEM/BEI images of transverse cross section confirm the change in grain morphology and size at the HAZ (Figure 10a-b). The periodic HAZ are circular ($\sim 100\ \mu\text{m}$ in diameter) and contains radially oriented columnar grains with pinholes at the HAZ center in many cases. The transverse and longitudinal images together suggest that the HAZ's most likely are 3-dimensional and trapezoidal extending through the film thickness. The columnar grains in the HAZ are oriented perpendicular to the plating direction in a radial fashion. Thin circumferential cracks were also found on the transverse cross-section SEM/BEI/SEI images (Figure 11). The cracks most likely correspond to the cracking seen at the deposit/cu-coated steel substrate interface shown in Figure 7a-b.

It should be noted that the presence of the dimples is an artifact due to underplating. They can be eliminated easily by overplating and lapping. An interesting consideration regarding the HAZ is that this periodic arrangement of HAZ cylinders in the Ni matrix is characteristic of a composite structure. Whether the HAZ's are beneficial or harmful to material properties and behavior is unclear and is a subject reserved for future evaluation. Pinholes were seen in the center of almost every HAZ on the etched side. The depth of the pinhole has not yet been examined and should be an important issue to address. These pinholes certainly affect the deposit integrity. It should be possible to eliminate or minimize the pinholes formation by optimizing the screen hole size relative to the substrate area.

Deposit Type III (3-Dimensional Ni Replication Mold/Substrate)

The electrodeposition in this case occurs on a solid Ni piece formed by electrodeposition into a Type I LIGA mold (Figure 12). The Ni is allowed to overplate and form a continuous thick film on top of the PMMA. The Ni piece, with the inverse topography of the original LIGA mold, is then inverted and used as a substrate for subsequent metal plating. The deposition thus occurs in 3-dimensions since the sidewalls are electrically active. If electrodeposition parameters are not carefully chosen to promote uniform feature filling, small cavities may form at the feature center as shown in the optical images in Figure 13a-c. The original intent of this approach was to attempt to mechanically separate the Ni parts plated into the Ni mold; this proved difficult, and this approach was replaced by a similar one using electrically conductive PMMA molds (see deposit Type IV below).

Macroscopic cavities were found in most features in the particular sample shown in SEM/BEI transverse cross-section (Figure 13c). The cavity appeared to be confined near the center without access to the surface as shown in longitudinal cross section (Figure 13a-b). The longitudinal cross-section also indicates the tendency of premature closure at the feature mouth (Figure 14a). This is especially true for higher aspect ratio features in the mold, where the deposit is in general much thicker near the mouth than the bottom due to a locally higher deposition rate.

The grain morphology and size derived from this mold are similar to those seen in the previous 2-D molds except for their multi-directional nature. The long axis orientation of the columnar grain is dictated by the cathodic sidewall location (Figure 14a-d). There are cell boundaries separating the columnar grains from those with different orientations, as evidenced by longitudinal and transverse

sections (Figure 14a-c). The individual grains are in general 2 μ m wide and 10 μ m long. Voids in the feature center appeared to be completely contained within the deposits.

Deposit Type IV (3-D Ag-Fiber-PMMA Mold/Substrate)

After difficulties with the mechanical separation step for deposit Type III, efforts were focused instead on PMMA substrates that were doped with Ag fibers for conductivity. These substrates are attractive since embossing or injection molding, imparting some desired pattern to the surface in either case, may be employed to form them. After electrodeposition, the substrate can be dissolved with acetone, eliminating the demolding step necessary for deposit Type III.

The samples used in this part of the study were underplated intentionally for electroplating process evaluation in a related investigation (Ref 2). Substrate molds are cylindrical, high aspect ratio (~100 μ m in diameter and 1mm in length) and mechanically drilled (Figure 15). The PMMA composite substrate is porous with pore sizes ranging from 100 to 500 μ m (Figure 16). The Ag-fiber density in general is uniform and consistent throughout the substrate (Figure 16b). The deposits plated on the sidewalls are approximately 10 μ m thick.

SEM/BEI images of longitudinal sections show the deposition is multi-directional and in most cases about 10 μ m thick on all sidewalls (Figure.17). The deposits appear to be much thicker at the substrate surface and feature mouth near the top. Two of the four features mouths appeared to be prematurely closed by the thick deposit (Figure 17, Mold c-d). Large open pores were seen along some features sidewalls (Figure 17, Mold b, c, and d). These open pores apparently were conductive enough for plating to commence, resulting in large amount of deposited Ni on the original deposit surface (Figure 17, Arrow B).

The deposit microstructure on the composite substrate is not as predictable as those seen in the previous cases. Grain structure is greatly affected by the substrate sidewall morphology, roughness, Ag-fiber density, and pore density. On the planar surface and smooth sidewalls, the grains are columnar and uniform as in deposit Type I. This is verified by the SEM/BEI images from both longitudinal and transverse x-section (Figure 18a-b). On the rough non-planar walls, the grain structure is highly irregular for the initial 5 μ m. Columnar and equiaxed grains are present in the same region (Figure 18c). After the initial 5 μ m, the grain structure returns to normal columnar.

IV. Summary

The main physical features of all four types of electrodeposited Ni are summarized in this section. Deposit Type I exhibits a consistent microstructure throughout the part dimension. Grains are columnar with an aspect ratio greater than 5, the long axis parallel to the film growth direction. Deposit Type II is composed of columnar grains directly above the steel substrate and radial columnar grains above the microscreen holes. Pinholes were evident in the center of most of the cylindrical regions containing the radial grains; these regions were presumably due to the presence of the insulating holes. Deposit Type III exhibits columnar grains pointing to the feature sidewalls and bottom since deposition occurs on all these surfaces. Voids, associated with deposition parameters that were not optimized, were present at the center of some features. For features that are not very deep ($<500\ \mu\text{m}$), the proper choice of pulse plating parameters should eliminate the voiding, leaving a center seam. The uniformity of deposit Type IV is affected by heterogeneity in the substrate, which is somewhat porous. Some large open pores ($\gg 20\ \mu\text{m}$) affect the geometry of the substrate sidewall, leading to variations in the thickness of the plated Ni film. Deposition in this composite substrate is also multi-directional as seen in deposit Type III. The microstructure is heterogeneous, depending on the substrate sidewall morphology, roughness, and local Ag-fiber density. Void formation is also evident in this deposit type for the same reason as in deposit Type III.

The implication of the above morphological characteristics on the metallurgical properties or material behavior is yet to be examined in all cases. It should be emphasized that the current results are collected from limited samples from still-evolving processes in Sandia National Laboratories, California. The objective of this communication is to report some interesting aspects of the physical structure of electrodeposited Ni arising from deposition on unique substrates. These results should be useful in future process development and optimization.

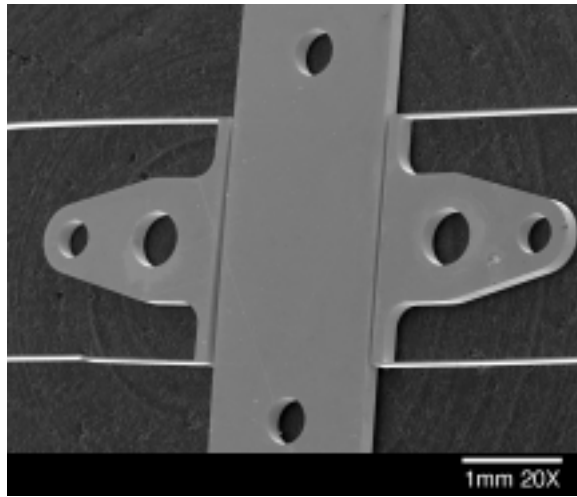
V. Conclusions

This study has identified important varying characteristics of electrodeposited Ni derived from four molding processes in development at Sandia National Laboratories, California. The results show that the microstructure and the film integrity are greatly affected by substrate molding material and its design configuration. The use of alternative substrates associated with these different molding processes may lead to Ni grain morphologies and structural imperfections that are not typically encountered in Ni deposited on planar, continuous substrates.

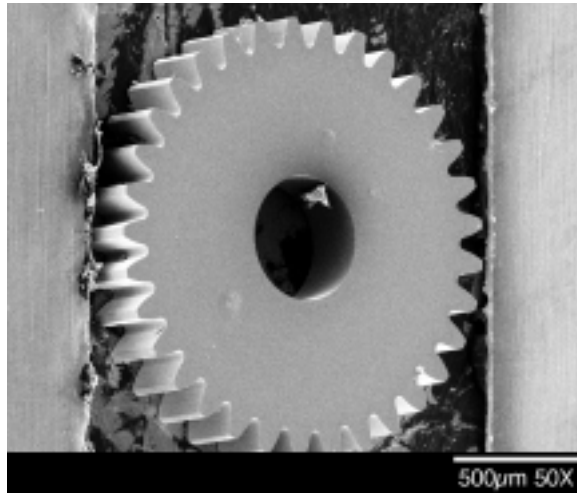
References

1. "Electrodeposition on Ni from a Sulfamate Electrolyte, Part 1: Effect of Stress Relief on Annealing Behavior and Film Metallurgy," J. J. Kelly and N. Y. Yang, SAND Report, SAND2001-8609, October 2001.
2. "Micro-Replication: Precision Metal Parts from Electroformed Master Molds," J. J. Kelly and N. Y. C. Yang, SAND Report, SAND2001-8732, January 2002.
3. "Microscreen Based Replication of Electroforming Micromolds," L. A. Domeier, M. Gonzales, J. T. Hachman, J. M. Hruby, R. P. Janek, A. M. Morales, *Microsystem Technologies* 8 (2002), p. 78-82.

Figures

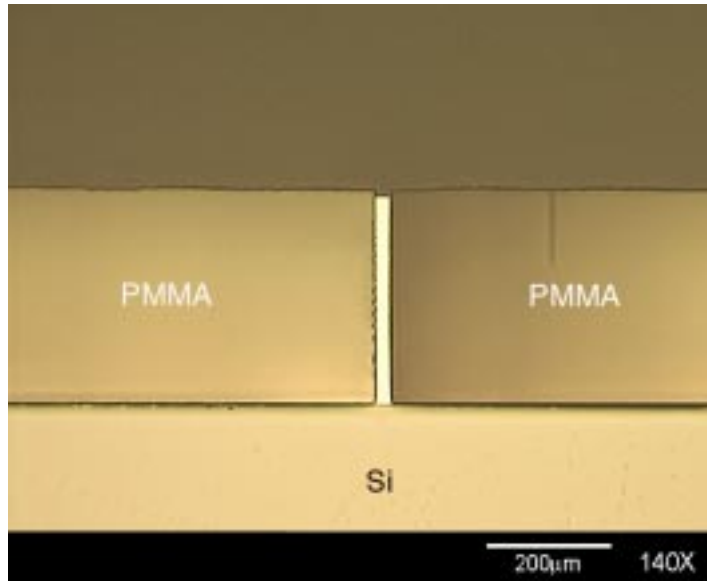


(a) ESD shuttle

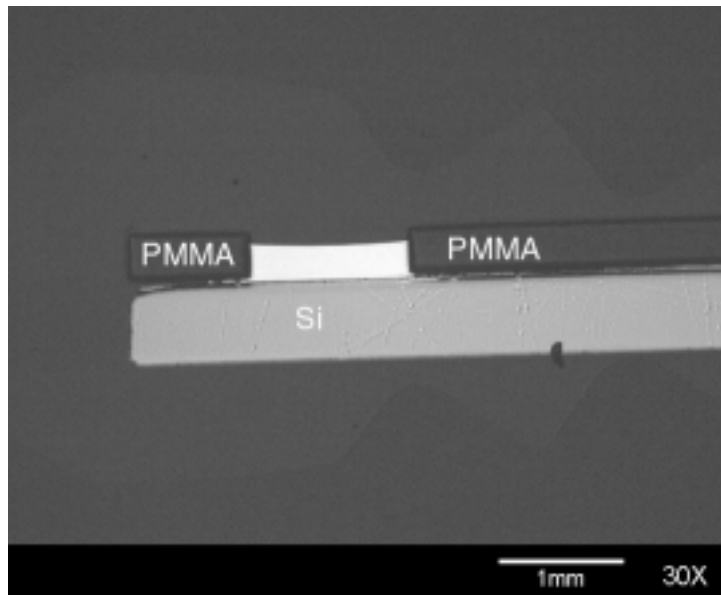


(b) Microgear

Figure 1. SEM/SEI images showing typical configuration and dimension of deposit plated from the PMMA-Ti/Cu/Ti substrate.



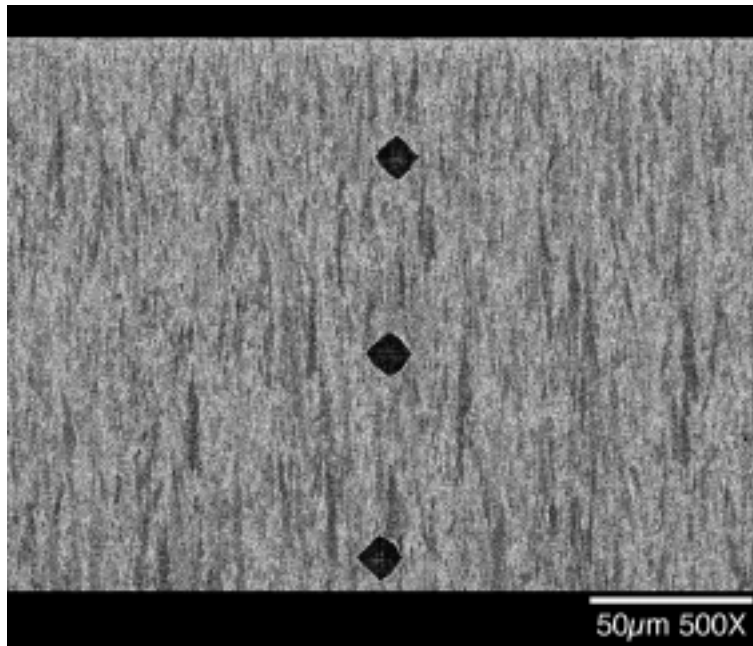
(a) High aspect ratio flexure



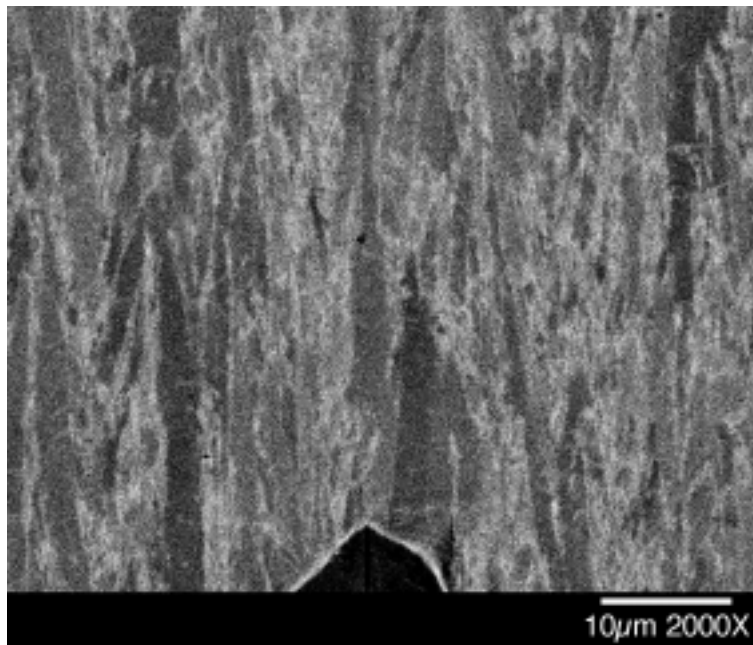
(b) Low aspect ratio body

↑
Plating
Direction

Figure 2. Optical images of longitudinal x-section of underplated ESD shuttle showing uniform thickness and void free deposits



(a) Full thickness at magnification of 500x.
(b)



(b) Near the PMMA/Cu interface at magnification of 2000x.

Figure 3. SEM/BEI images of longitudinal x-section showing typical columnar grains plated from PMMA-Ti/Cu/Ti substrate. Dark diamond features in the micrographs are artifacts of indentations from hardness test.

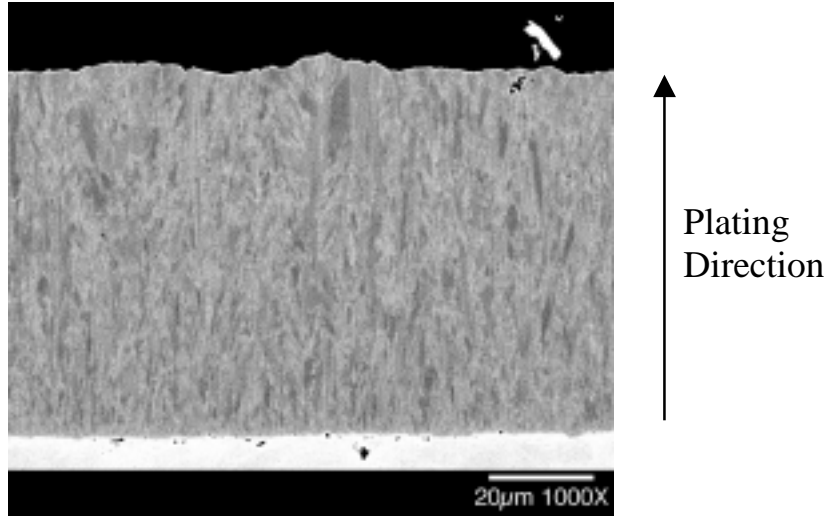
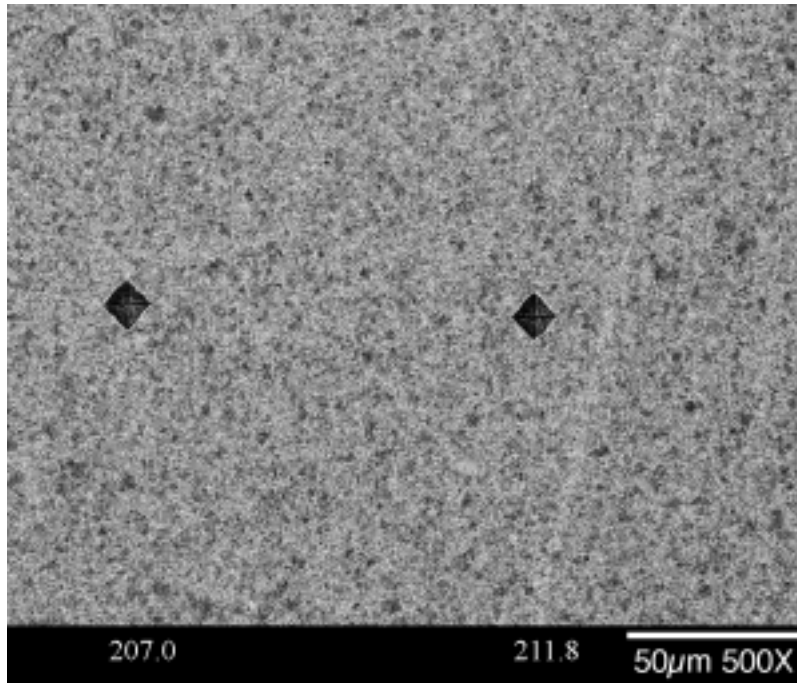
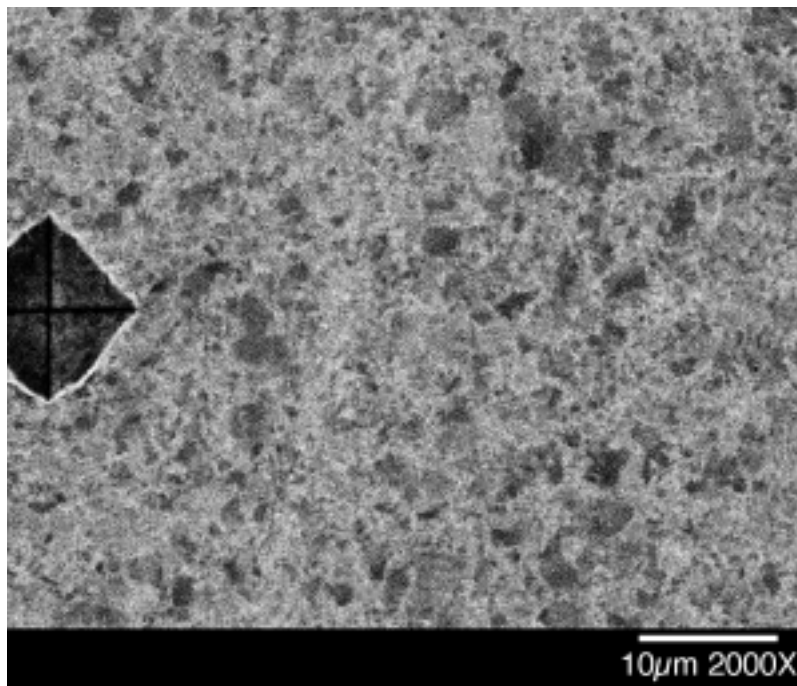


Figure 4. SEM/BEI image showing columnar grain size increase toward the top surface.

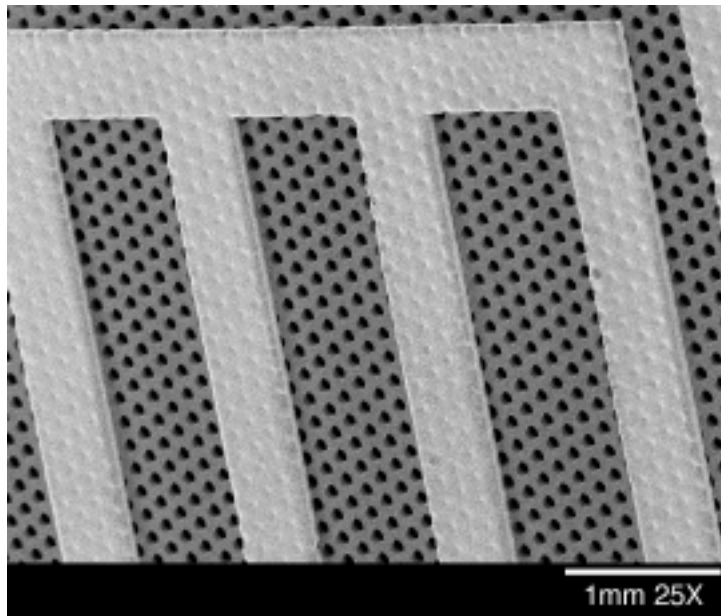


(a) At magnification of 500x

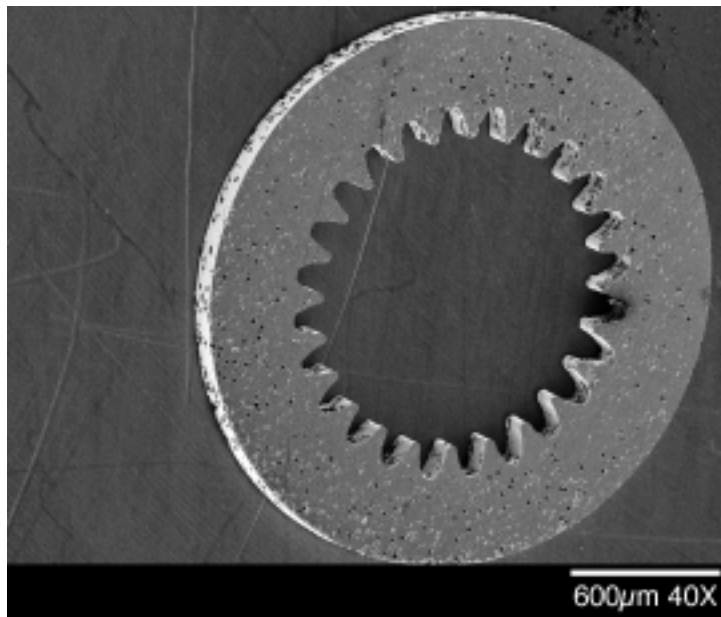


(b) At magnification of 2000x

Figure 5. SEM BEI images of transverse x-section showing typical equiaxed grains plated from PMMA-Ti/Cu/Ti substrate.

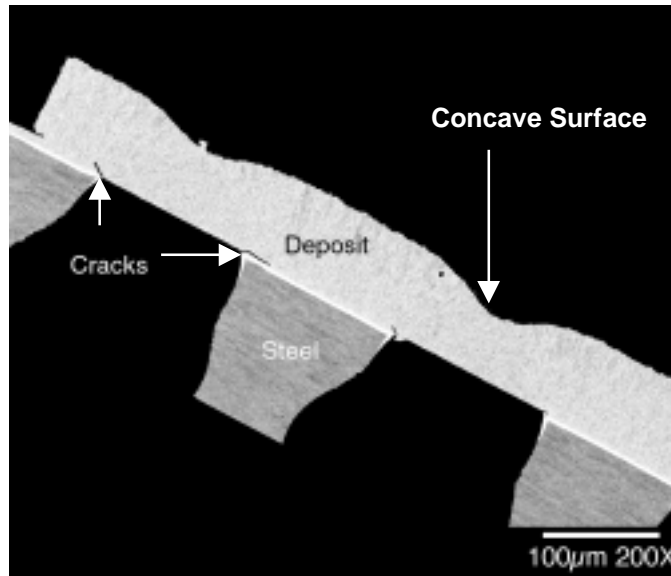


a. Unreleased/underplated test pattern

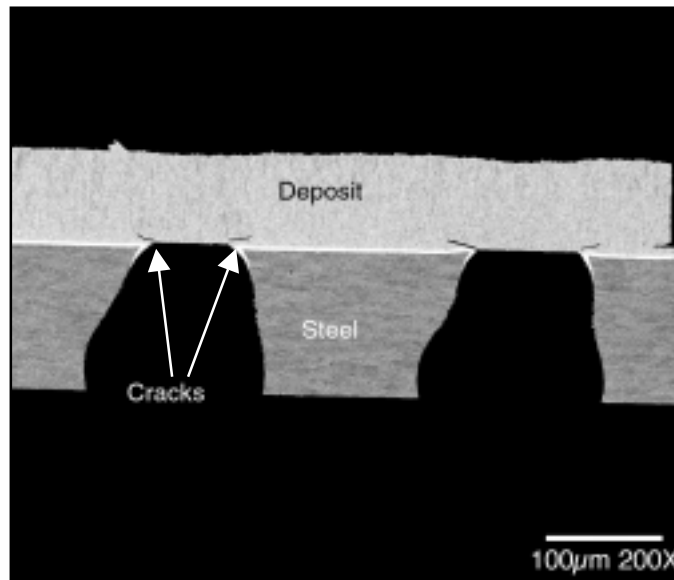


b. Overplated/lapped/released gear

Figure 6. SEM/SEI images showing the typical configuration and dimension of test patterns plated from PMMA-steel microscreen substrate.

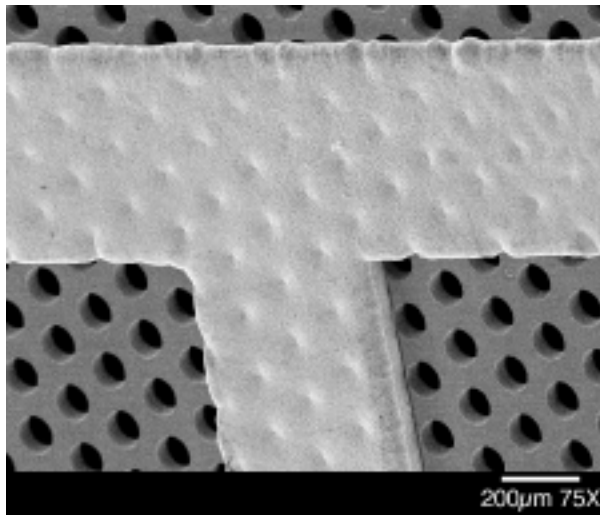


(a) Thickness above the steel substrate or near the hole edge is uniform without pore.

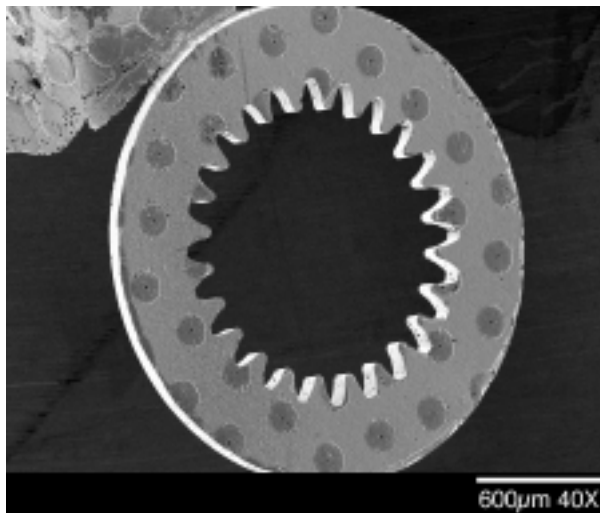


(b) Deposits surface above the holes are concave.

Figure 7. SEM/BEI images of longitudinal x-section showing deposit density and thickness variation throughout the substrate. Cracks were found along many deposit/substrate interfaces.



(a) Periodic dimples were found on the top surface, above the holes.



(b-c) Periodic circular disks with a pinhole in the centers were found on the released surface, above the holes.

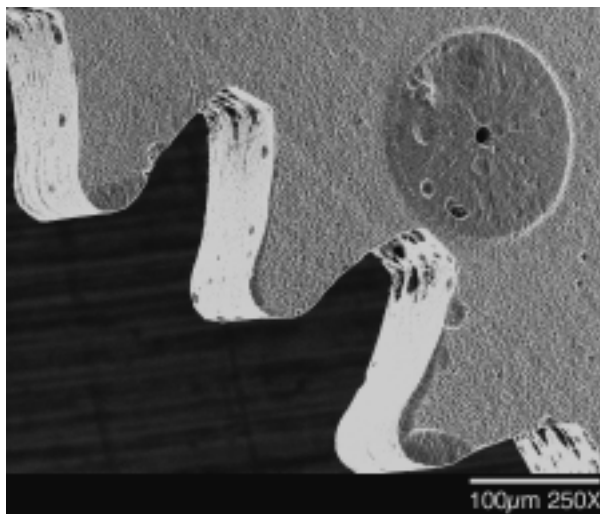
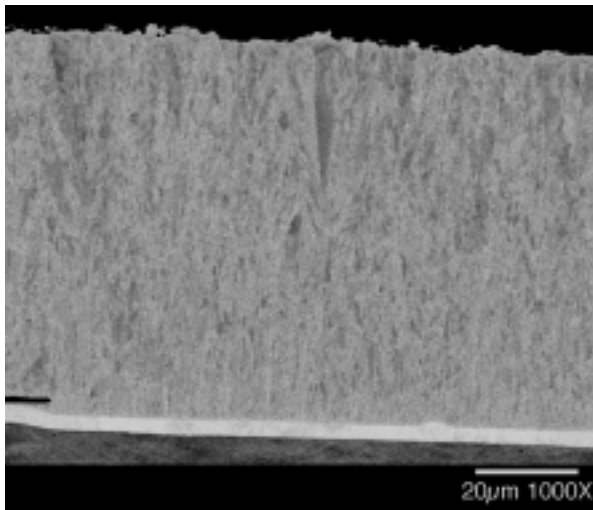
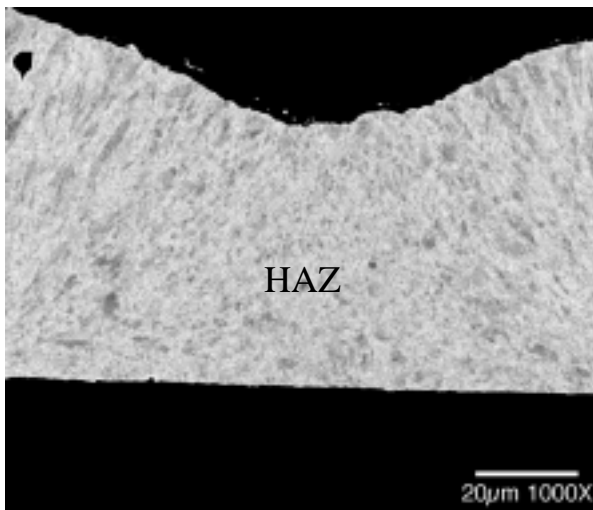


Figure 8. SEM/SEI images of as-received underplated surface showing effect of insulating holes on the deposit integrity.



(a) Unidirectional columnar grains were seen above the steel substrate.



(b-c) Long axis of columnar grains slanted towards the center of the holes and the surface is concave. Concave depth is highly dependent on distance from the hole.

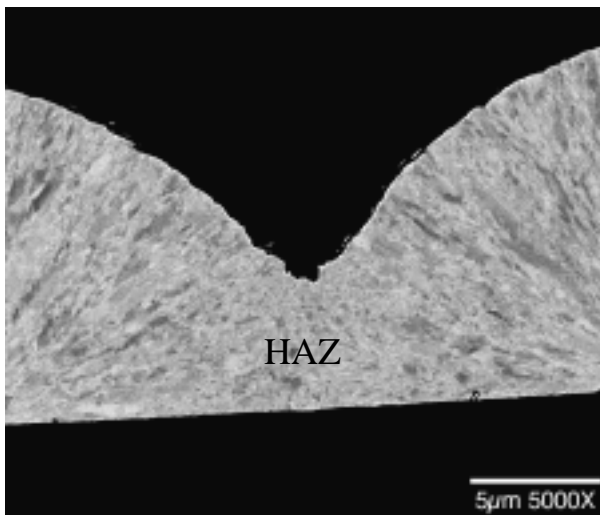
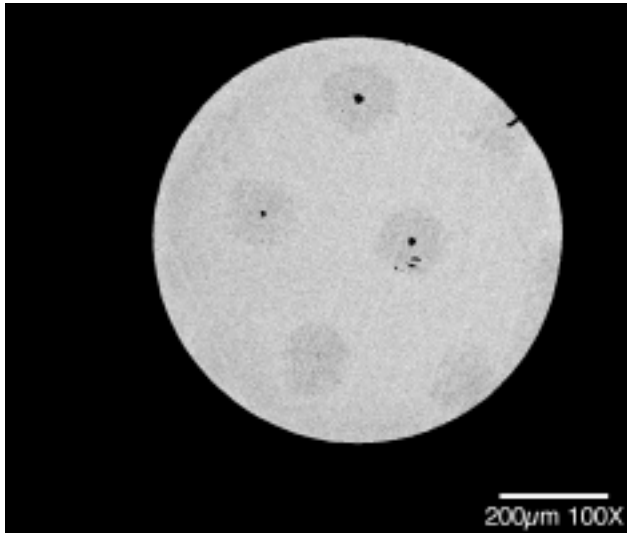
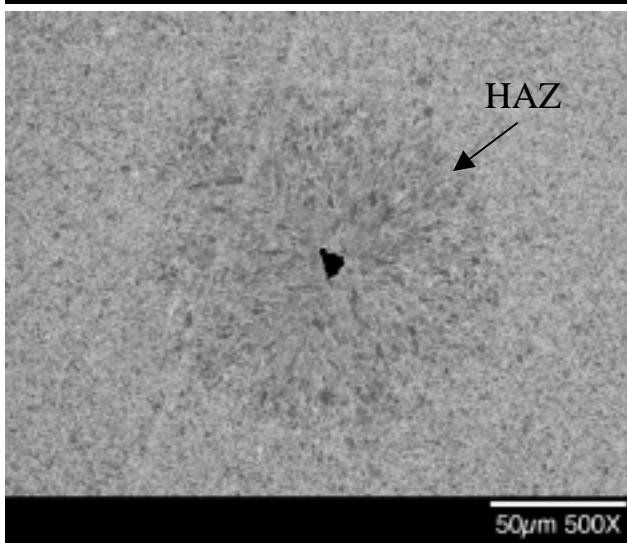


Figure 9. SEM/BEI of longitudinal x-section showing microstructure of the deposits plated from the PMMA-steel microscreen substrate.



(a) Above the holes, there are periodic HAZ (~100 μ m in diameter) with a pinhole in the centers.



(b-c) Columnar grains are radial oriented toward the pinholes.

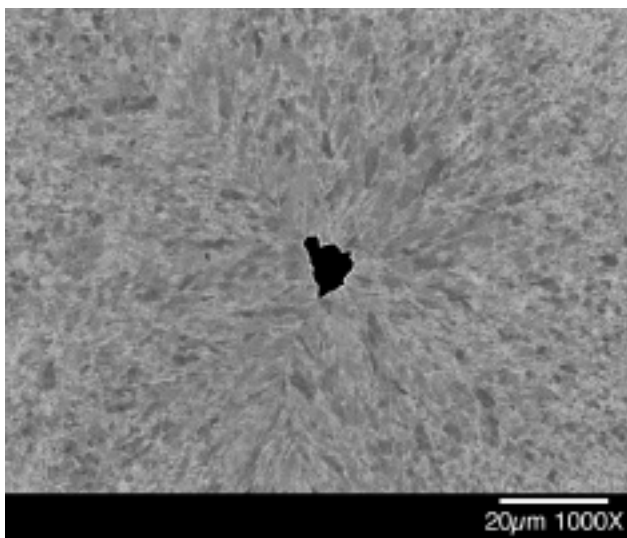
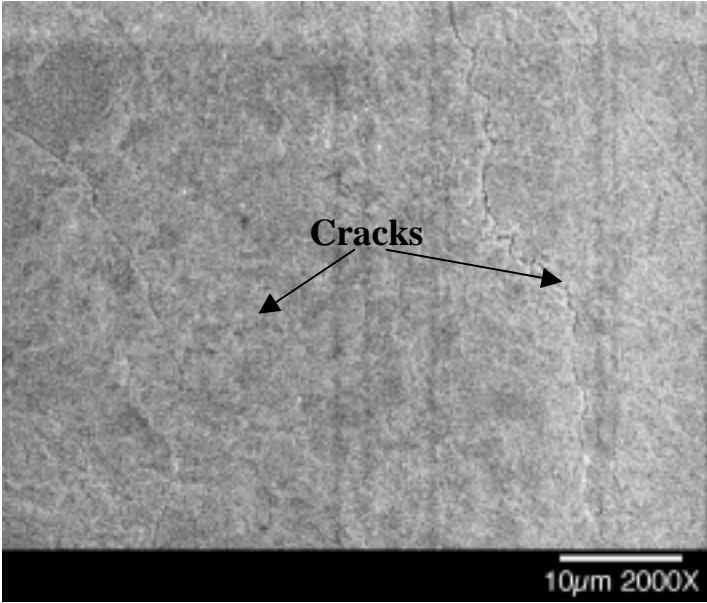
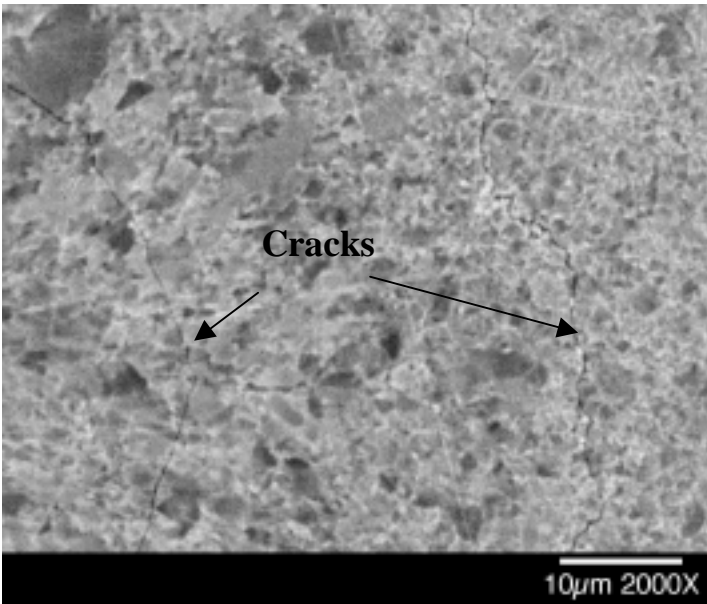


Figure 10. SEM/BEI of transverse x-section showing typical microstructure of deposit on a round pattern.



(a) SEM/SEI image.



(b) SEM/BEI image.

Figure 11. Cracks found along the HAZ circumferential boundaries.

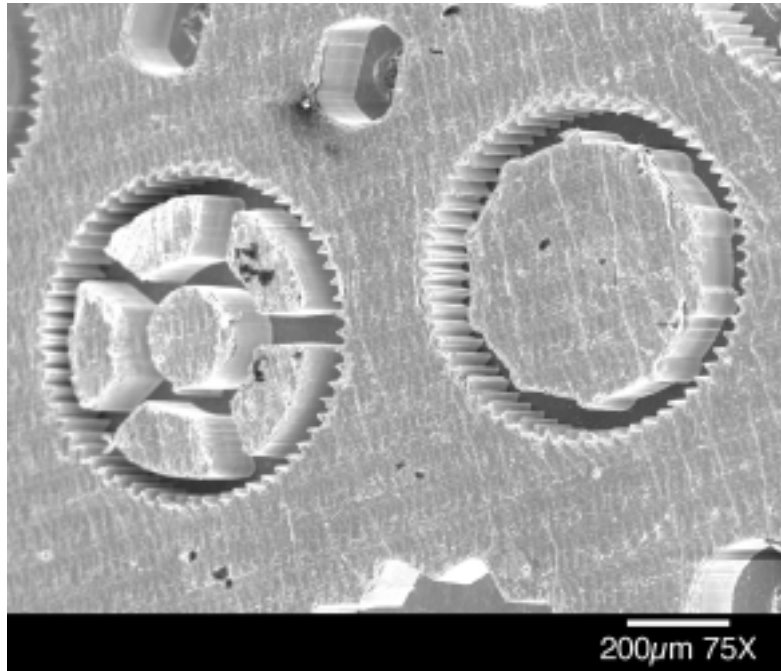
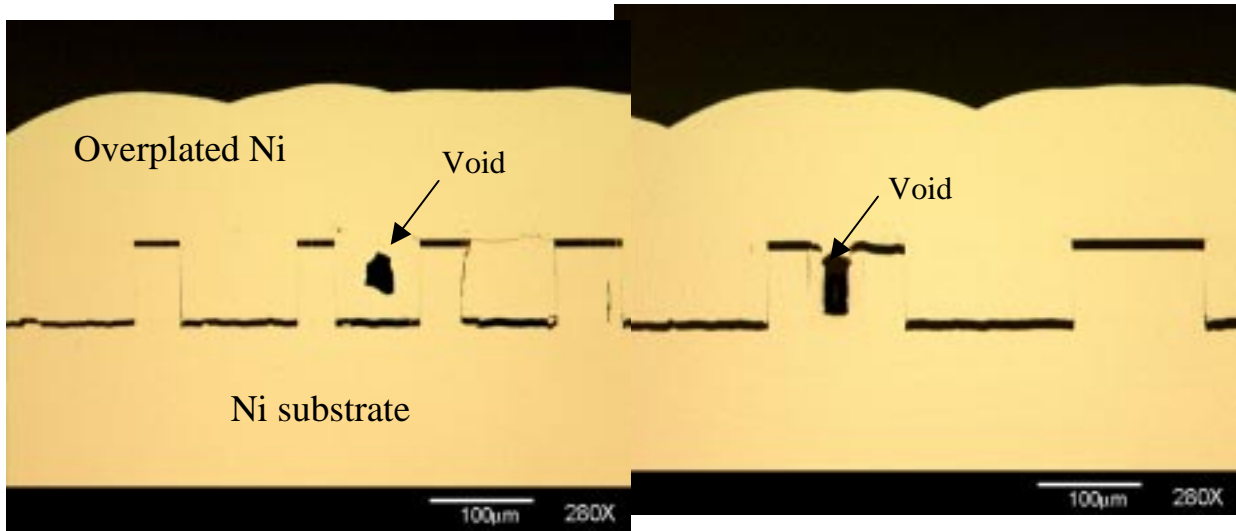
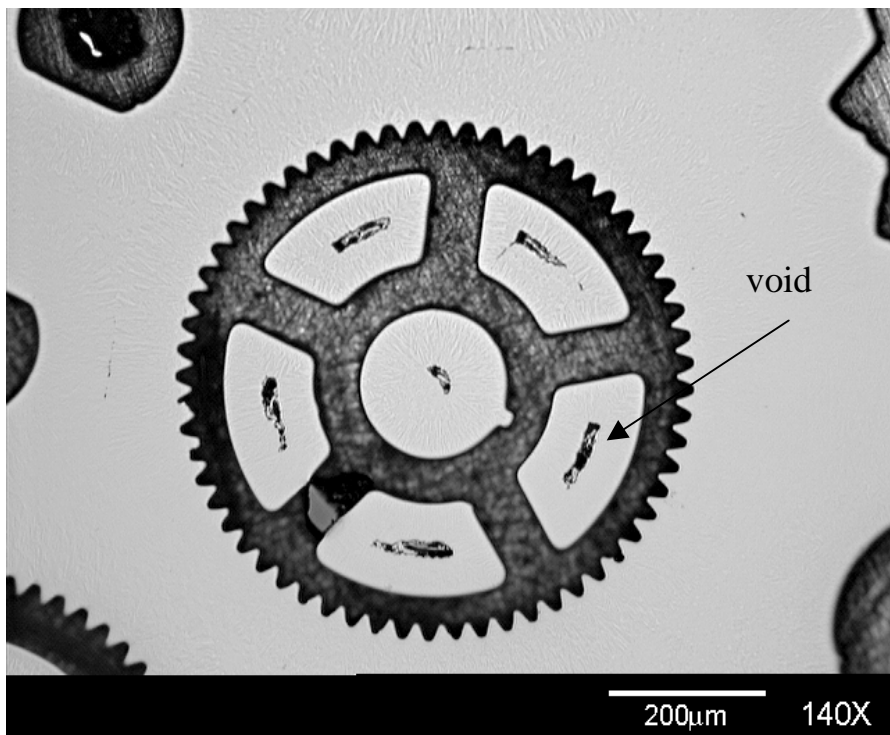


Figure 12. SEM/SEI images showing the surface morphology and dimension of mechanically released test patterns. Thin wavy cracks on the surface are artifacts due to the mechanical removal of the parts from the substrate.

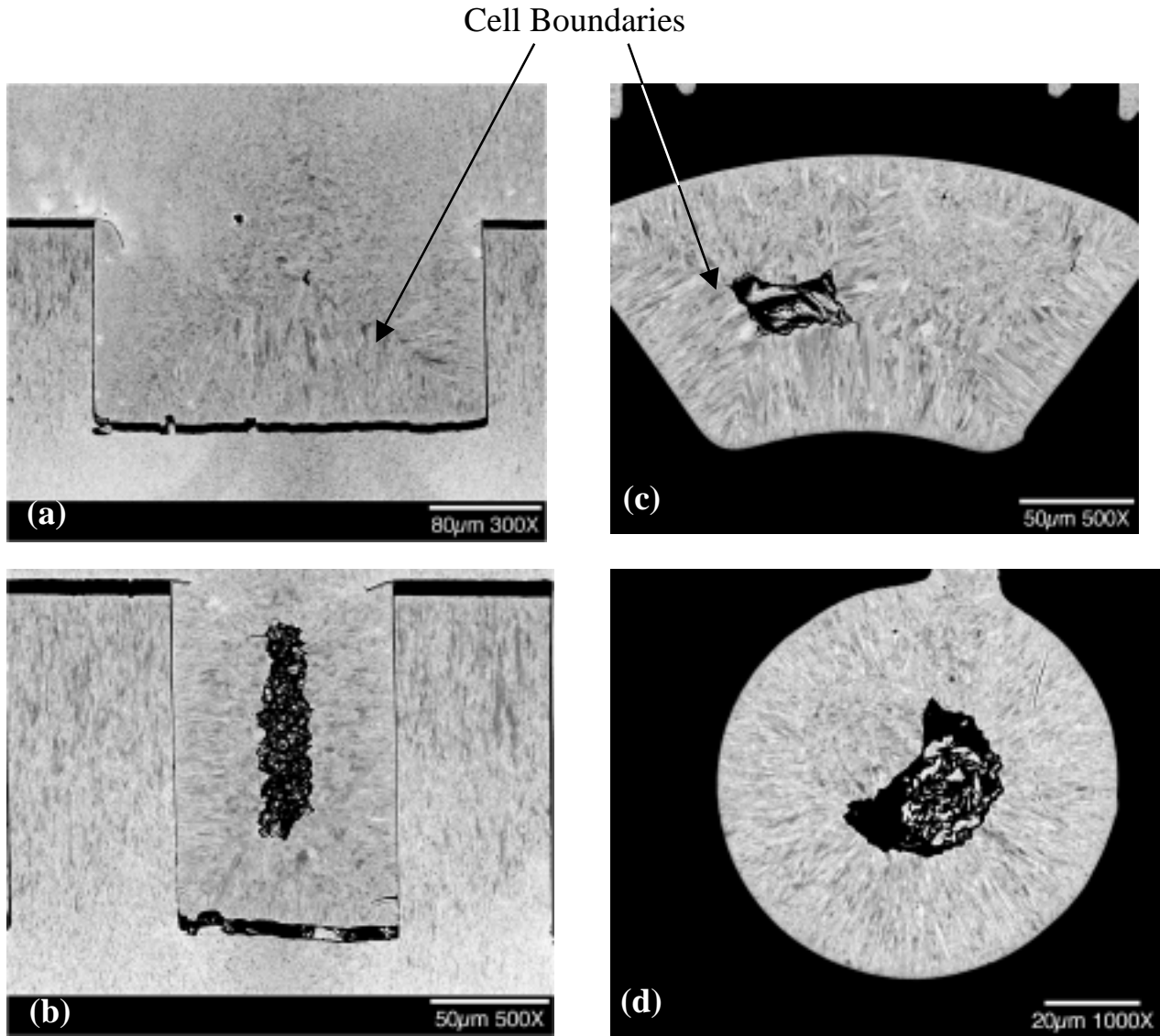


(a-b) Longitudinal x-sections show voiding in the center of some test patterns.



(c) Transverse x-section shows voids seen in the center of all the test patterns.

Figure 13. SEM/BEI image of test pattern x-section showing the deposit density and integrity.



(a-b) Longitudinal x-section

(c-d) Transverse x-section

Figure 14. SEM/BEI images of the x-sections showing multi-directional deposition and microstructure of the deposit plated from the Ni-substrate. Columnar grains with different orientations were separated by cell boundaries. Large voids are also evident.

Mechanically drilled molds

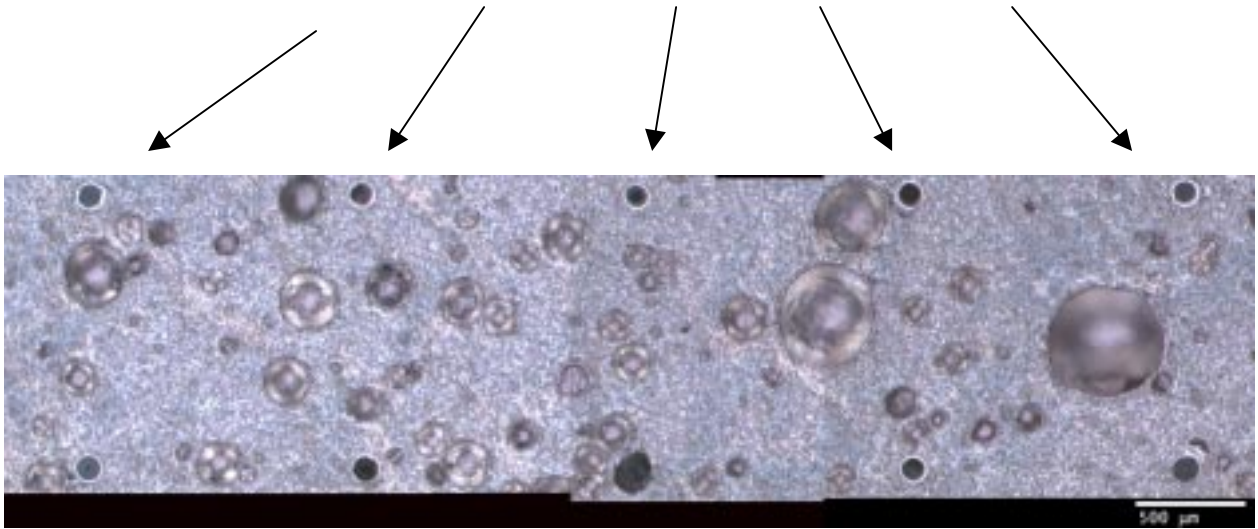


Figure 15. Optical images of as-received substrate surface showing underplated deposits on the mechanically drilled molds (see arrows). Spherical pores (100 μm to 500 μm) were seen on the substrate surface.

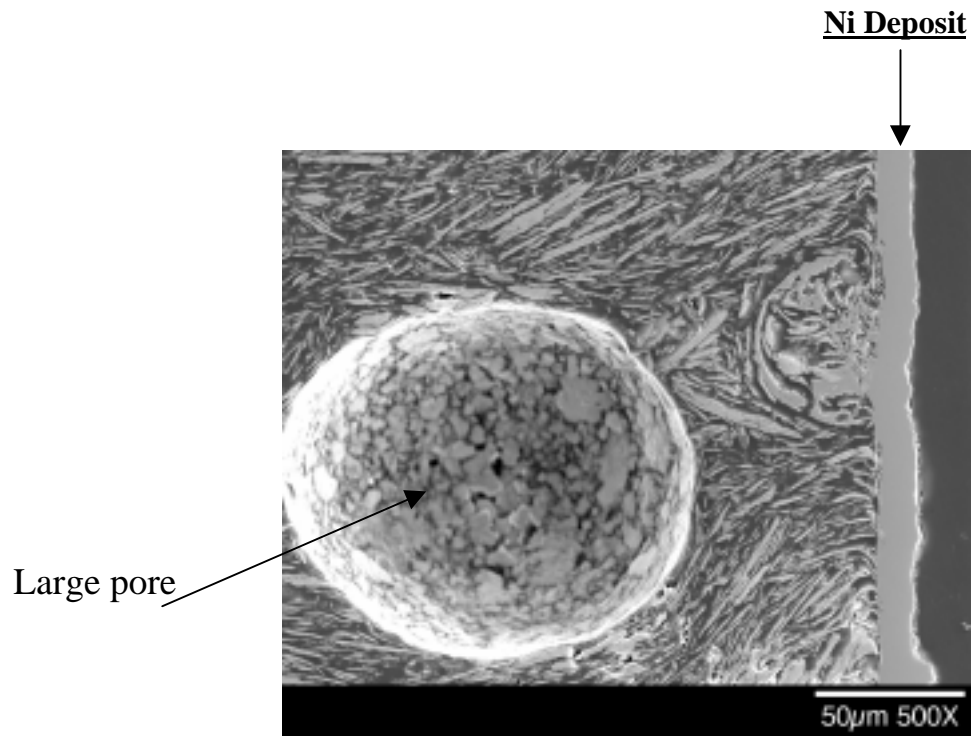
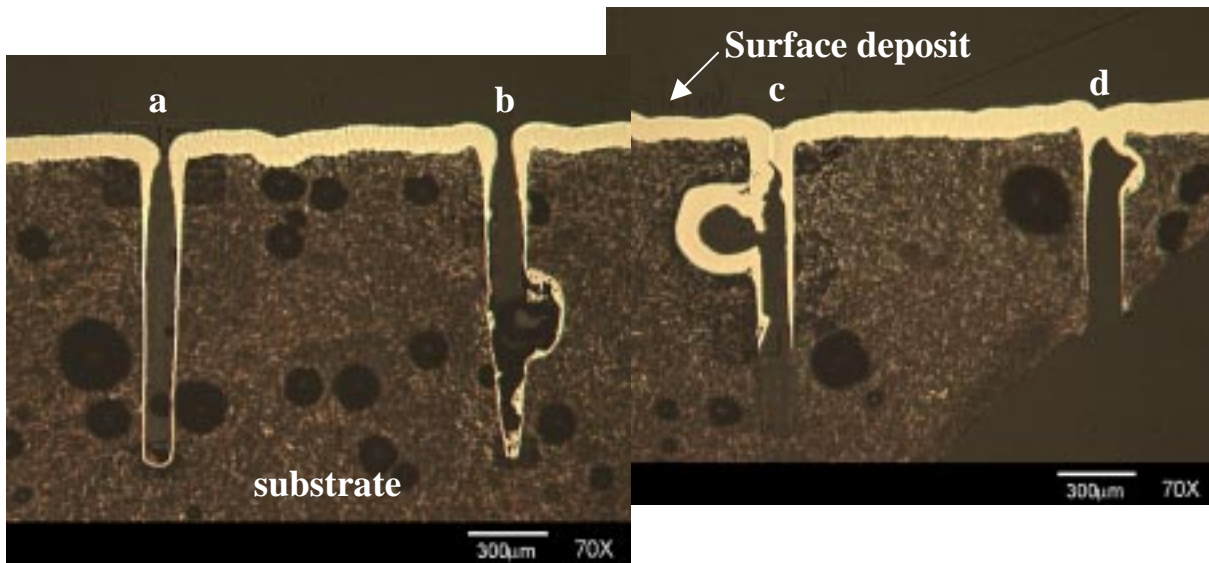
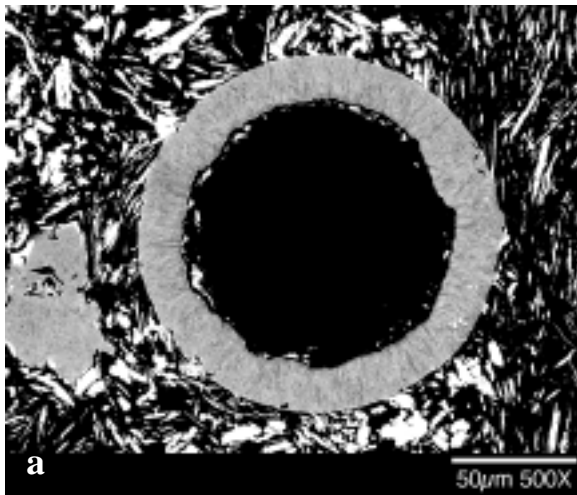


Figure 16. SEM/SEI image of longitudinal x-section showing microstructure of the Ag-fibers and pores.

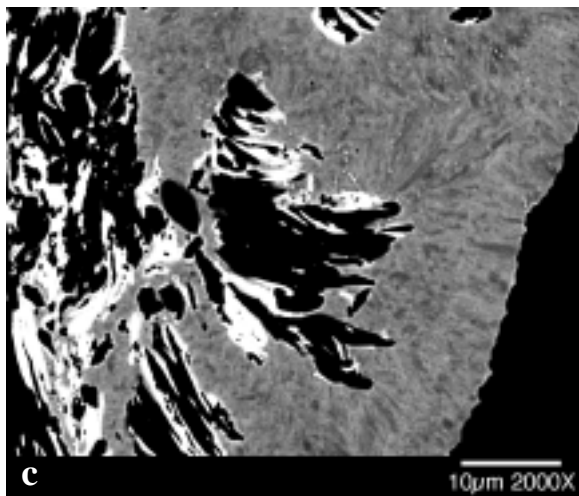
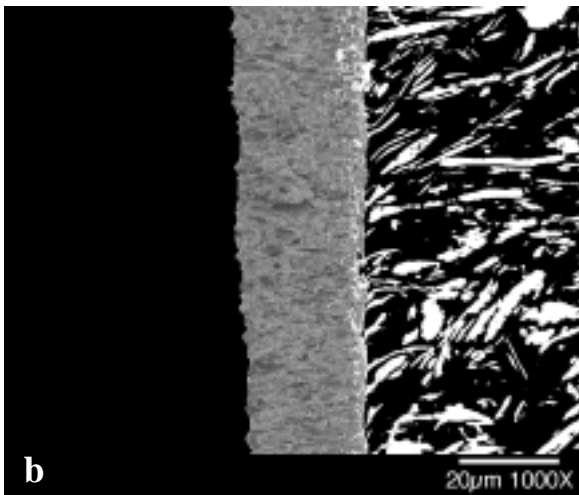


- Mold (a) The deposit thickness appeared to be uniform on all walls.
- Mold (b-d) Large open pores with thick Ni-deposit were seen on the sidewall.
- Mold (c-d) Features mouths close prematurely by thick deposit. Deposit is missing at the bottom.

Figure 17. Optical image of the longitudinal x-section showing typical deposit thickness variation in the molds and the substrate. Deposit on the substrate top surface and near the feature mouths are much thicker than those in the molds.



(a-b) Uniform columnar grains on the smooth planar sidewall.



(c) Irregular morphology of the initial 5µm on the rough non-planar sidewall.

Figure 18. SEM/BEI image of longitudinal x-section showing microstructure of the deposit plated on the Ag-fiber-PMMA mold.

UNLIMITED RELEASE

INITIAL DISTRIBUTION

1	MS0139	R. Kreutzfeld, 2613	MS9161	R. Q. Hwang, 8721	
1	MS0329	L. L. Lukens, 2614	MS9402	C. H. Cadden, 8724	
1	MS0329	M. A. Polosky, 2614	MS9403	W. R. Even, 8722	
1	MS0139	C. W. Vanecek, 2613	MS9404	J. R. Garcia, 8725	
1	MS0889	B. L. Boyce, 1835	MS9409	J. Goldsmith, 8730	
1	MS0889	T. E. Buchheit, 1835	MS9409	G. D. Kubiak, 8732	
			MS9409	W. C. Replogle, 8731	
1	MS9001	M. E. John, 8000; Attn:	3	MS9018	Central Technical Files, 8945-1
	MS9002	P. N. Smith, 8500	1	MS0899	Technical Library, 9616
	MS9003	K. E. Washington, 8900	1	MS9021	Classification Office, 8511/ Technical Library, MS0899, 9616
	MS9004	J. Vitko, 8100			
	MS9031	K. C. Olsen, 11600			
	MS9054	W. J. McLean, 8300			
1	MS9042	J. A. Crowell, 8727			DOE/OSTI via URL
1	MS9042	S. K. Griffiths, 8728			
1	MS9042	W-Y Lu, 8725			
1	MS9042	B. Nilson, 8728			
1	MS9401	J. M. Hruby, 8702			
1	MS9401	G. Aigeldinger, 8729			
1	MS9401	M. A. Bankert, 8729			
1	MS9401	J. T. Hachman, 8729			
1	MS9401	C. C. Henderson, 8729			
5	MS9401	J. J. Kelly, 8729			
1	MS9401	D. E. McLean, 8729			
1	MS9401	A. M. Morales, 8729			
1	MS9401	F-J Pantenburg, 8729			
1	MS9401	D. M. Skala, 8729			
1	MS9401	C-Y P. Yang, 8729			
1	MS9402	K. L. Wilson, 8724			
1	MS9403	J. C. Wang, 8723			
10	MS9403	N. Y. C. Yang, 8723			
1	MS9403	L. Domeier, 8722			
1	MS9403	B. Simmons, 8722			
1	MS9404	S. H. Goods, 8725			
1	MS9405	D. A. Hughes, 8726			
1	MS9671	D. A. Chinn, 8729			
1	MS9405	R. H. Stulen, 8700; Attn:			
	MS9042	A. R. Ortega, 8727 (Actg.)			
	MS9042	M. F. Horstemeyer, 8728			
	MS9161	E. P. Chen, 8726			